International Journal of Engineering and Manufacturing Science.
ISSN 2249-3115 Volume 7, Number 2 (2017), pp. 203-224

http://www.ripublication.com

A Review on Aluminium Based Metal Matrix Composites by Friction Stir Processing

[1,2]D.S.Chandra Mouli
[1]Research Scholar, Dept. of Mechanical Engg, JNTU, Kakinada, India.
[2]Asst. Professor, Dept. of Mechanical Engg, Malla Reddy Engg. College, Hyderabad.

[2]R. Uma Maheswara Rao
Professor of Mechanical Engg Dept, Sasi Inst. Of Technology & Engg, Tadepalligudem, India.

[3,4]A. Sarath Kumar
[3]Research Scholar, Dept. of Mech Engg., K L University, Guntur, India.
[4]Asst. Professor, Dept. of Mech Engg, Malla Reddy Engg. College, Hyderabad.

Abstract

Metal matrix composites are recently developing modern engineering materials where the surface microstructure of the material is modified by reinforcing secondary material in the form of powder particles or fibers into the base materials and the characteristics of core effect without any changes in compositions. Many aluminum alloys with specific properties, like high strength, suffers from certain limitations in terms of cost and time of production. The various applications of Al MMCs can be found in automotive, aerospace, biomedical and power industries.

Nowadays, a technique like Friction Stir Processing (FSP) has been using in producing surface composites in solid state itself. Al and its alloys being difficult to process metals also have been successfully processed by FSP to change their Properties effectively. The present paper is to give a comprehensive summary on fabrication of Al based composites by FSP.

Influence of the secondary phase material and microstructure refinement resulted from stirred technique on *the materials' properties is also discussed.*

Keywords: Friction stir processing, Aluminium MMC and Grain Refinement etc.

1. INTRODUCTION

Aluminum and its MMCs have wide range of applications especially in the fabrication industries, aircraft manufacturing, automobile body building, shipbuilding and other structural applications, due to their high strength to weight ratio, higher ductility and good corrosive resistance. Metal matrix composites (MMCs) are a significant group of modern engineered materials that have clearly demonstrated their potential as promising candidates for various structural applications [1].By adding some amount of secondary phase particles, The specific strength of the base metal or pure metal can be improved. Aluminum, copper, magnesium and titanium are a few examples for matrix materials and SiC, SiO_2, Al_2O_3, TiB_2, WC are a few examples for secondary phase materials. And Stir casting [2], squeeze casting [3-5], spray deposition [6], *in situ* fabrication [7], powder metallurgy [8-10], diffusion bonding [9] and vapor deposition methods are a few examples for manufacturing techniques commonly used to fabricate bulk MMCs [11-13]. Recently Al and its alloys have proven as excellent candidates for constructing structures in various industries like automobile, aerospace, marine, biomedical and electronic industries because of their high strength weight ratio, And also high strength accompanied by high ductility is possible with materials having fine and homogeneous grain structure. Aluminum based MMCs are an upcoming new class of materials in non-ferrous metals that address the problems associated with ductility of Aluminium. As mentioned above industries facing problems in some important applications in which the surface properties affect the functioning and the life of the component. Surface MMCs are the right examples for such type of materials, which reinforced by secondary material particles into primary composition without effecting the core properties. Therefore the surface exhibits more hardness, strength and wear resistance in some cases. To fabricate the surface effectively laser assisted processes, centrifugal casting and plasma spraying are a few examples of such methods developed to fabricate surface MMCs [15-20]. All of these techniques involve the material transformation from solid to liquid or vapor state during the process. On the flipside, there are another technique like solid state processing that do not result in transformation of metal to liquid phase during the process. They offer relatively many benefits over previously mentioned.

Friction surfacing and friction stir processing are the best example of that techniques used to modify the surface to develope the MMCs.

FSP expands the innovation of friction stir welding (FSW) developed by The Welding

Institute (TWI) of United Kingdom in 1991 to develop local and surface properties at selected locations. FSP is a new and unique thermo-mechanical processing technique that alters the microstructural and mechanical properties of the material in a single pass to achieve maximum performance with low production cost in less time. FSP offers many advantages over the conventional and also the newer techniques of material processing which include being a single step process, use of simple and inexpensive tool, no expensive time consuming finishing process requirement, less processing time, use of existing and readily available machine tool technology, suitability to automation, adaptability to robot use, being energy efficient and environmental friendly.

In Friction stir process (Fig. 1), a specially designed cylindrical tool is used which while rotating is plunged into the selected area of sheet. The tool has a small diameter pin with a concentric larger diameter shoulder. When the tool is plunged into the sheet, the rotating pin contacts the surface and friction between the sheet surface and the shoulder rapidly heats and softens a small column of metal, enabling the transverse movement of the tool through the material. The tool shoulder and length of the probe control the depth of penetration. During FSP, the area to be processed and the tool are moved relative to each other such that the tool traverses, with overlapping passes, until the entire selected area is processed to a desired (fine) grain size. The probe is typically slightly shorter than the thickness of the work piece and its diameter is typically the thickness of the work piece. The processed zone cools as the tool passes, forming a defect free, and The microstructure in the weld nugget zone evolves through a continuous dynam-ical recrystallization process and the strong grain refinement produced by the process leads to fine dimensions of the microstructure and then to the possibility of exhibiting higher mechanical properties.

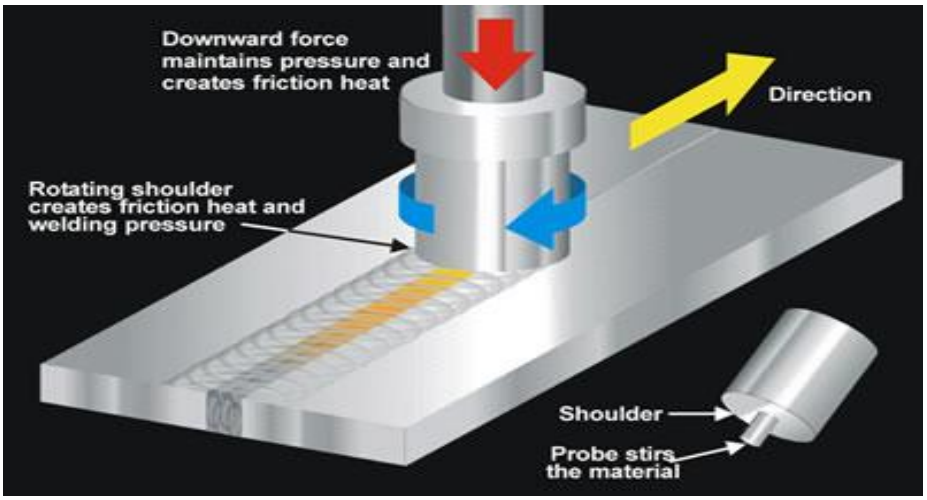

Fig. 1. Schematic illustration of friction stirs processing

2. LITERATURE REVIEW

P.cavaliere (2006) performed friction stir processing to enhance the surface properties of Al 2014-Zr alloy. This investigation dealt the effect of FSP on the tensile strength and fatigue properties of Zr modified 2014 aluminium alloy. The alloy used by cavaliere had the following chemical composition (wt%): Cu= 4.32, Mg= 0.49, Zr= 0.12, Si= 0.68, Fe= 0.23, Mn= 0.77,Ti= 0.03, Al= bal.; The material is taken in the form of extrude rods 80mm in diameter, from that center of the billet 3mm-thick and 50mm-long square sheets were cut parallel to the extrusion direction. the material was friction stir processed in same direction of extrusion. The nib of the tool was 6 mm in diameter and 2.8 mm long. A 20-mm diameter shoulder was machined perpendicular to the axis of the tool with a tilt angle of the tool of 3°. The rotating speed of the tool was 1000 rpm, while the travelling speed was 2.67 mm/s. the addition of transition elements such as Zirconium by FSP was resulted by forming trialuminides with low solubility and low diffusion coefficient provides a very useful instrument in the control of the microstructure aluminium alloy. the secondary phase particles develop a large coarsening resistance in the matrix in addition to high thermal stability due to their higher melting point with respect to the matrix[28-30]. the Zr modified 2014 Al alloy specimens were sectioned in longitudinal direction along the processing line with an electric discharge machine (EDM) to test the tensile strength of stirred zone. the tests were conducted on MTS 810 testing machine at room temperature with initial strain rate of 10^{-3} s^{-1}. the endurance fatigue test were performed on a resonant electro-mechanical testing machine

(TES-TRONICTM 50 ± 25 kN, produced by RUMUL, SUI) under constant loading control up to 250 Hz with sine wave loading. The cyclic fatigue tests were conducted in the axial total stress–amplitude control mode under fully reversed, push–pull, tension loading ($R = \sigma_{min}/\sigma_{max} = 0.1$). The geometry of the specimens used is shown in fig.2.

Fig. 2: Macrograph of the specimens used for fatigue tests

Table 1: Room temperature tensile properties of 2014+Zr aluminium alloy in the FSP and as-received conditions.

Material	yield strength(MPa)	UTS(MPa)	Strain to fracture
2014+Zr FSP	440	650	0.16
2014+Zr	410	600	0.14

According to cavaliere, Due to the presence of Zr particles in the form of spherical and coherent Al_3Zr precipitates in a cubic form after FSP, the micorstructure was modified at very fine grain level effectively. And it was observed by the FEGSEM and TEM inspection of the as-received Zr-modified material revealed the presence of very fine precipitates within the grains as expected as shown in (Fig. 3).

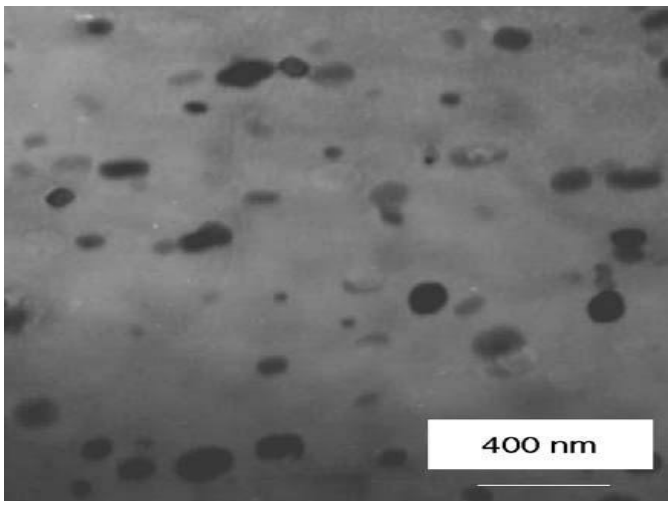

Fig. 3: Al_3Zr precipitates observed in the studied material

The optical microscopy observations performed on the cross-section of the stirred samples revealed the classical onion structure, “nugget” zone characterized by very fine equiaxed grains as shown in Fig. 4, surrounded by the thermo-mechanically affected zone and by the heat-affected zone. The nugget zone is characterized by very fine equiaxed grains produced during the continuous dynamic recrystallization process acting during FSP.

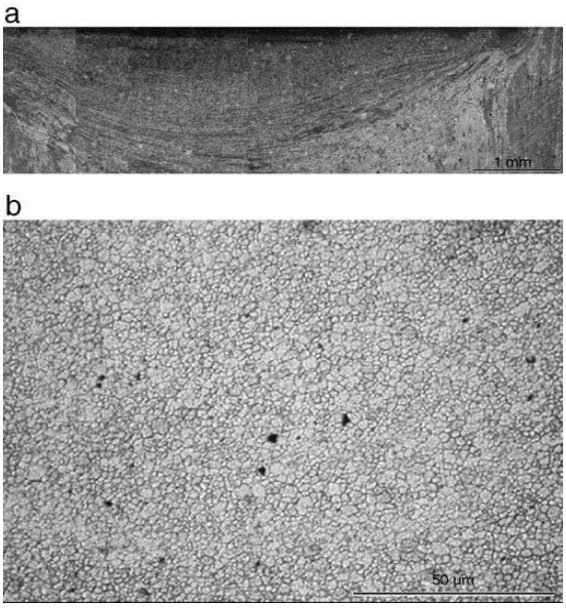

Fig. 4: Macrograph of the stirred zone (a) and Nugget zone equiaxed recrystallized grains after the dynamic recrystallization process (b).

The room temperature tensile response of the FSP material is reported in Table 1, and the results are compared with those obtained from the parent material. The FSP material exhibits a net increase in strength accompanied with a lower increase in ductility. The curve representing the stress amplitude–fatigue life response of the material in longitudinal direction is reported in Fig. 5. The curve shows a classical behaviour revealing a trend of increasing fatigue life with decreasing cyclic stress amplitude.

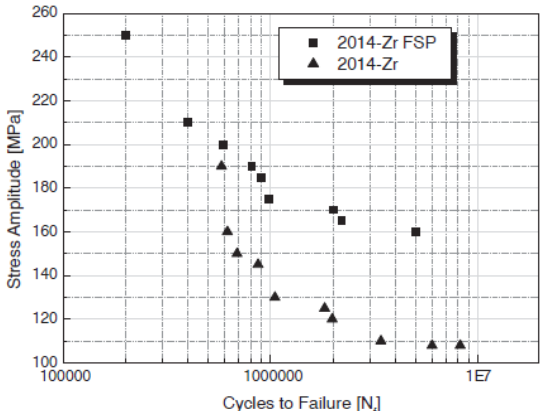

Fig. 5: Fatigue endurance S–N curve of the studied material in FSP and as-extruded conditions.

In both low and high cycle regimes, the material failure was characterized by small regions of stable microscopic crack growth. The high ductility of the material during cyclic loading was revealed in both low and high cycle regimes shown in Fig. 6a, b. In both regimes, isolated small zones of striation-like features shown in Fig. 7a, b and the presence of local ductility in the zones surrounding the small voids were observed in Fig. 8a&b.

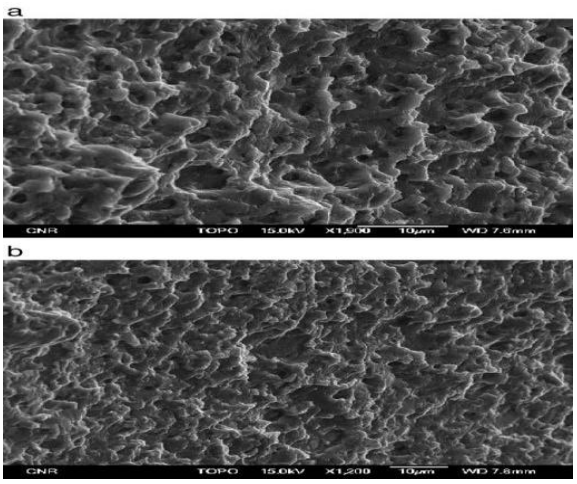

Fig. 6. Fracture surfaces of the specimens tested in fatigue at 210 (a) and 160 (b) MPa stress amplitude

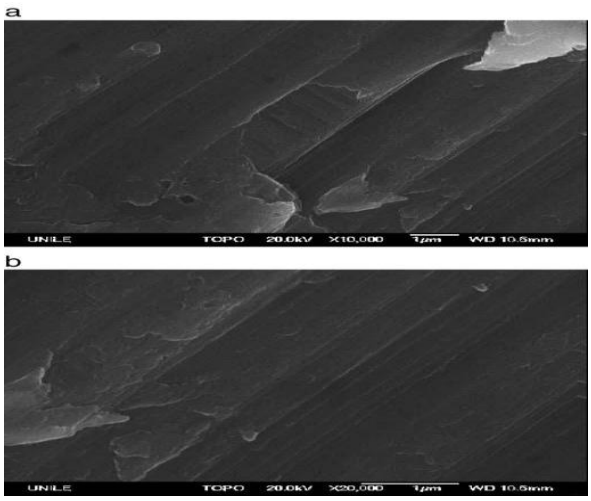

Fig. 7. Fine fatigue striations observed on the fracture surface of the specimens tested at 210 (a) and 180 (b) MPa.

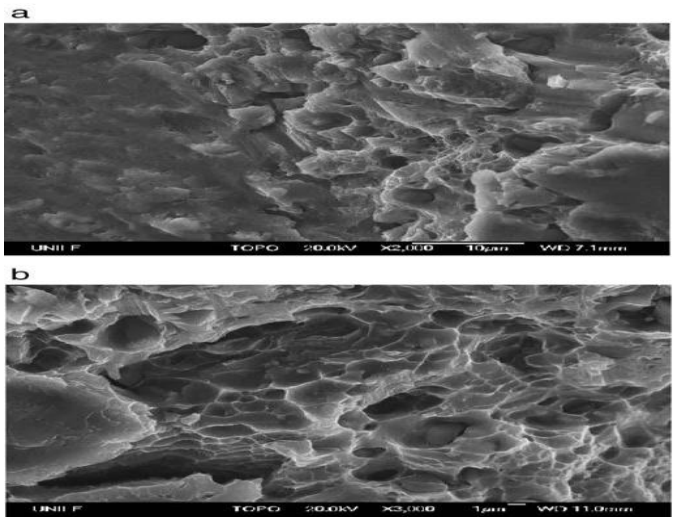

Fig. 8. Very fine dimples observed at higher magnifications on the fracture surfaces of the specimens tested in fatigue at 210 (a) and 160 (b) MPa stress amplitude

A.THANGARASU et al (2012) investigated the effect of FSP on microstructure and microhardness of the AA1050 with TiC (~2 μm) as secondary phase material reinforced into the primary material. Commercially pure (98.2%) 1050 aluminum which had iron(0.40%), silicon(0.25%), manganese(0.13%) and copper(0.05%) as major impurities was chosen as matrix material in the form of 10 mm thick plate. The measured content of TiC powders were compacted into a groove of 0.5 mm × 5.5 mm. A single pass FSP was carried out using a tool rotational speed of 1600 rpm, processing speed of 60 mm/min and axial force of 10 kN. A tool made of HCHCr steel, oil hardened to 62 HRC, having a cylindrical profile of tool had a shoulder diameter of 18mm, pin diameter of 6mm and pin length of 5.8mm. to fabricate the Al metal matrix composite. Fig 9 shows the upper surface appearance of the fabricated surface metal matrix composites(SMMCs).

Fig. 9. Crown appearance of FSP zone of AA1050/TiC SMMC.

Defects such as voids and cracks are not observed on the surface and the surface shows very smooth surface quality without any depressions while tool stirring. From the Fig. 10 A defect free FSP zone is observed due to sufficient groove size completely bonded on all sides. The pin length is 0.3 mm higher than that of the groove depth which proves to be adequate to produce full penetration. Fig 11 shows the interface zone at the retreading side between the base metal and FSPed metal, Thermo mechanically affected zone(TMAZ) is observed and exhibits the distribution of TiC particles along parallel bands in the Al matrix. Fig 12 (a &b) shows the FSP zone of Al matrix ,The obviously refined grain size of Al alloy and homogenously distributed TiC particles in FSP zone causes to attain the higher mechanical properties in SMMCs.

Fig. 10. Macrograph of FSP zone.

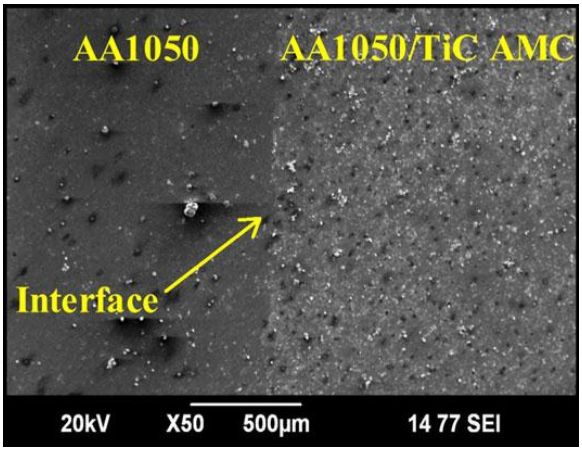

Fig. 11. SEM photomicrograph of interface zone.

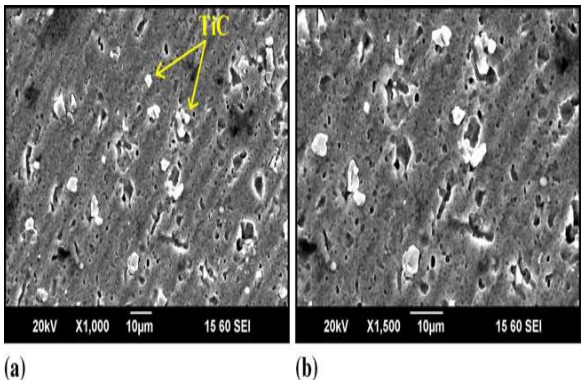

Fig. 12. (a) and **(b)** SEM photomicrograph of AA1050/TiC SMMC.

The microhardness of the base alloy by reinforcement the TiC particles is shown in Fig 13.The average hardness of FSP zone is 45% higher than that of the aluminium alloy. the major contributions to the hardness of the surface composite layer fabricated by FSP are is Orowan strengthening due to the fine dispersion of TiC particles and good bonding to matrix alloy. The peak hardness is observed away from the center at the advancing and retreating sides. The material flows in a complex fashion from the retreating to the advancing side during FSP giving rise to gradients in temperature, strain and strain rate across the stir zone. This in turn gives rise to different microstructural features at different locations in the stir zone. Moreover, since a groove was made at the center of the aluminum plate to incorporate the TiC particles, the material has to flow into the groove to fill it to give a defect-free continuous stir zone. Therefore, the center may experience less deformation compared to the sides. This may also be responsible for the hardness drop at the center.

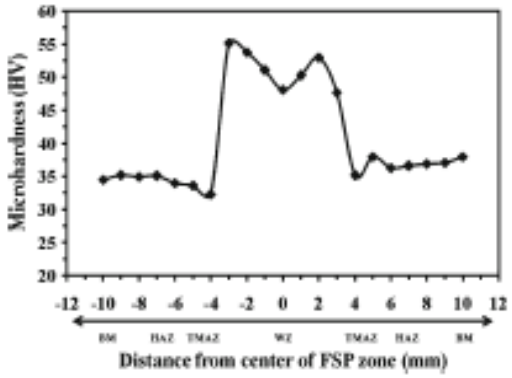

Fig. 13. Microhardness distribution in the base metal and composite.

Chi-Hoon Jeon et al (2014) studied the reinforcement of aluminium matrix with graphene in the form of graphene oxide(GO,1nm and 1-3μm)/water colloid with the

help of FSP to enhance the property thermal conductivity. The thermal conductivity of the graphene/ aluminum MMC is measured to increase by more than 15% in comparison with that of the aluminum matrix, and also improved ductility of the fabricated MMC. . One method to enhance the thermal conductivity of aluminum alloys while maintaining their light weight is fabricating metal matrix composites (MMC) using materials with extremely high thermal conductivity as reinforcement. Graphene is a basic building block for various graphitic materials including zero-dimensional fullerenes (C60), one-dimensional carbon nanotubes (CNT), and three-dimensional graphite. Graphene shows excellent thermal conductivity (~5.30×10^3 W/mK),[31] charge carrier mobility (~2×10^5 cm^2/ Vs),[32] intrinsic strength (~130 GPa), Young's modulus (~1.0 TPa),[33] and surface area (~ 2600 m^2/g).[34] Due to its excellent thermal conductivity, graphene is a good candidate for the reinforcement of an aluminum matrix to enhance the thermal conductivity. FSP is used to fabricate graphene/Al MMC ,4mm thick 5052-H32 aluminium alloy sheets with process parameters of rotation speed 700rpm, travel speed 70mm/min and plunge depth 3.1mm with a tool profile of concaved shoulder diameter of 20mm, pin diameter and length 6mm and 3mm. GO was applied directly to the surface of the metal matrix in the form of a GO/ water colloid (15 mg/ml) prior to FSP, as shown in the schematic of the suggested process Fig. 14.

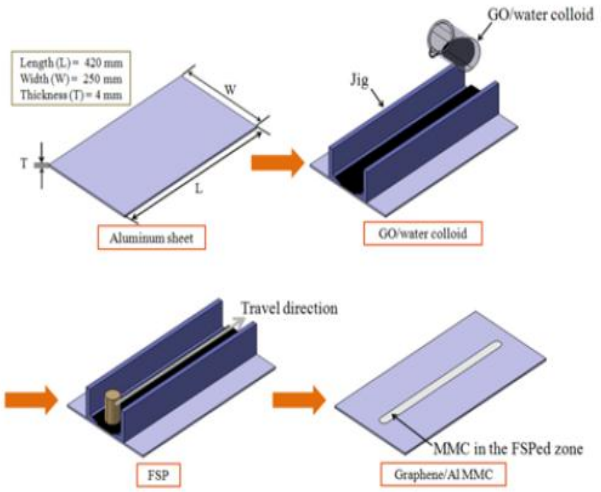

Fig. 14. A schematic of MMC fabrication by FSP

FSP of the aluminum 5052-H32 alloy sheet covered with GO/water colloid was successfully conducted without any noticeable macroscopic defects, as shown in the macroscopic top view in Fig. 15(a) and the cross-sectional optical micrograph in Fig. 15(b). The Raman spectrum of the GO was measured using a Raman spectrometer (DXR Raman microscope, Thermo Fisher Scientific Inc., USA) with incident laser

light at a wavelength of 633 nm. The Raman spectrum of the GO in Fig. 16(a&b) shows two apparent peaks at ~1328 and ~1595 cm^{-1}, corresponding to the D-band and G-band of graphene,[25] respectively. The Raman spectra of the stir zone suggest that GO reinforcements were well dispersed into the stir zone. The thermal conductivity evaluation shows that the thermal conductivity of the aluminum matrix was improved by more than 15% at 250°C by fabricating graphene/Al MMC (Table 2).

Table 2:

	Thermal conductivity* (W/mK)	Tensile strength** (MPa)	Elongation at failure** (%)
Aluminum 5052-H32	147.644 (0.66)	218.16 (2.64)	18.6 (2.86)
Aluminum 5052-H32, FSP alone	150.020 (0.74)	206.21 (3.05)	26.5 (2.98)
Graphene/Al MMC	171.698 (0.87)	191.99 (0.46)	28.0 (0.85)

*average of five measurements at 250°C; **average of four specimens; values in the parenthesis are the standard deviations.

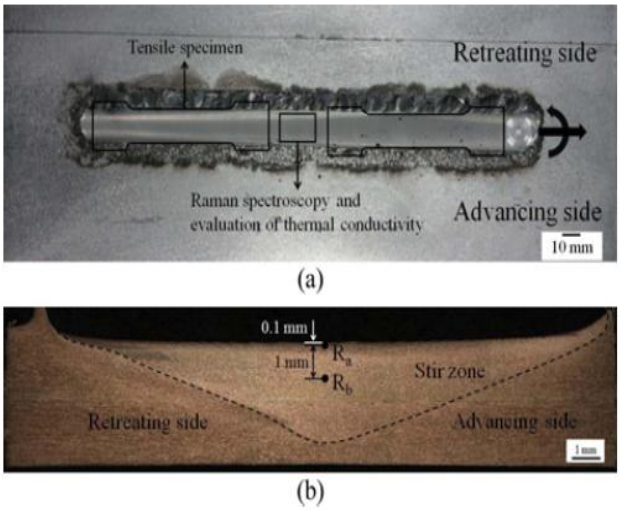

Fig. 15 (a). A macro top view and **(b).** a cross-section optical micrograph of the graphene/Al MMC

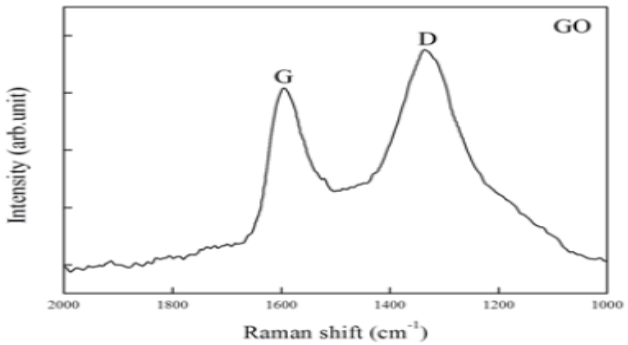

(a)

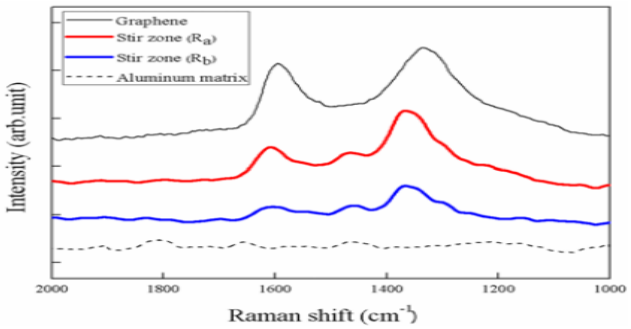

(b)

Fig. 16a. Raman spectrum of GO and **16.b** Raman spectrum of Graphene /Al MMC

The significantly improved thermal conductivity of the graphene/Al MMC confirms that the GO in the colloid was effectively reduced into highly conductive RGO by the heat generated by the friction and plastic work during FSP. The representative results of quasi-static tensile testing shown in Fig. 17 indicate that FSP significantly enhanced the ductility and slightly reduced the tensile strength of the aluminum 5052-H32 alloy. It is interesting to note that the ductility of the aluminum matrix, which was already significantly improved by FSP alone, was improved even more by the addition of graphene. An additional benefit of using FSP in the fabrication of MMC is that the ductility of the MMC can be significantly improved due to the grain refinement by FSP. A drawback of the suggested fabrication process is that the volume fraction of graphene reinforcement in MMC may not be precisely quantified even though the volume fraction of graphene reinforcement in MMC can be surely and easily increased by applying FSP with GO/water colloid multiple times to the same region of the matrix.[37]

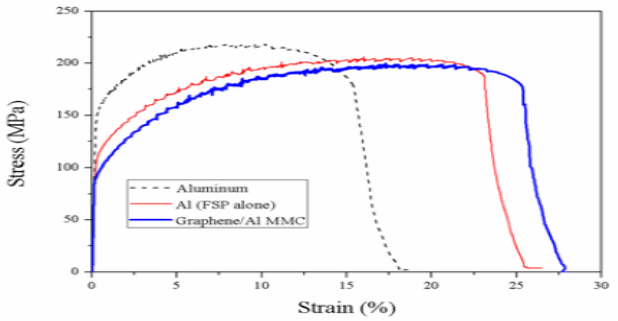

Fig 17. Representative engineering stress-strain curve of the graphene/Al MMC under quasi-static tensile loads

P.R GURU et al (2015) Investigated the effects of FSP on Al-Si cast alloy (LM25) for enhancement of the microstructure, mechanical properties and machinability. Age hardening response of as received cast alloy and friction stir processed alloy on machinability and mechanical behavior was also investigated. Aluminum–Silicon (Al–Si) cast alloys are widely used in auto-motive applications because of their low cost, low density, high temperature capability, and excellent castability. The dimensions of Al-Si plates were taken in this study as 8mmx60mmx310mm. These plates were friction stir processed (FSPed) at different rotation speeds (800 rpm to 1400 rpm), traverse speeds (60 mm/min to 150 mm/min) and plunge forces (4 kN to 9 kN). Among the various pilot experiments, the optimum rotation speed, traverse speed and plunge force was identified as 800 rpm, 120 mm/min and 9 kN, respectively. And the tool having cylindrical pin following diameter, length and shoulder diameter were 5.5 ± 0.2 mm, 4.5 ± 0.2 mm and 15 ± 0.3 mm.

The influence of FSP on mechanical behavior was studied by con-ducting microhardness and tensile testing on the cast and FSPed alloys. The samples for microhardness testing were prepared by grinding and polishing to create a flat and parallel surface. The test load and dwell time during microhardness testing was taken as 200 gf and 5 s, respectively. The samples for microhardness testing were taken from the transverse section of the processed area at the middle of the plate thickness. To determine tensile properties, mini-tensile specimens were prepared from the nugget region of the FSP zone along the FSP direction with the gage length and gage width of 4 mm and 2 mm, respectively. These tensile tests were conducted by using computer controlled Instron 3365 machine at a cross head velocity of 1 mm/min at room temperature. The fracture surfaces of tensile specimens were examined in a scanning electron microscope (SEM) for fractography study. A vertical CNC milling machine with force dynamometers were used to conduct drilling tests without applying cutting fluid in order to study the influence of FSP on machinability. A two flute HSS drill bit with shank diameter of 3 mm and 135° point angle was used for conducting drilling experiments with The following feed rates ranging from 0.15 mm/rev to 0.25 mm/rev. and cut-ting speeds (45–60 m/min) on both cast and FSPed alloys with and without peak ageing treatment.

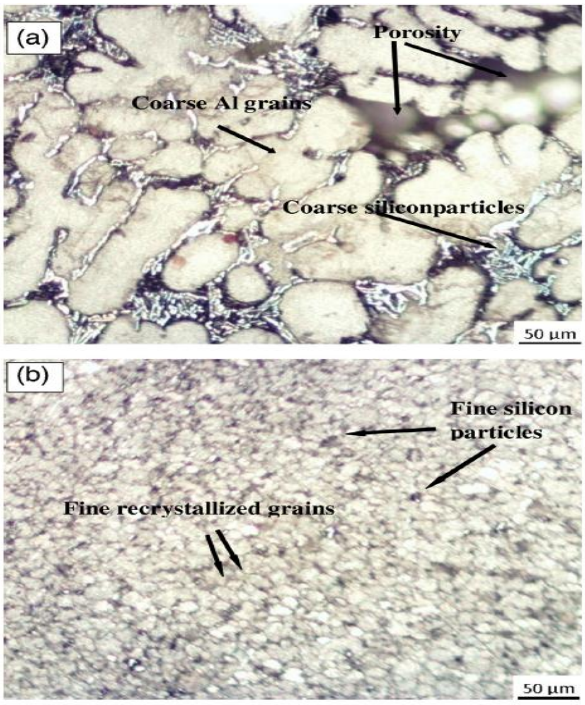

Fig. 18 Optical micrographs of (a) cast LM25 alloy (b) FSPed LM25 alloy.

Fig.18 (a) shows the microstructure of the as-cast LM25 alloy which contains primary α-Al dendrites and inter-dendrite irregular Al–Si eutectic regions. Coarse acicular Si particles are distributed along the primary Al boundaries, which indicate the non-uniform distri-bution of Si particles throughout the Al matrix. Furthermore, micro porosity up to ∼10.33% is detected in the as-cast LM25 plates. The influence of friction stir processing on microstructural evolution of cast LM25 alloy is illustrated in Fig.18(b). FSP resulted in a significant breakdown of coarse and acicular Si particles and Al dendrites, and also created an uniform distribution of fine and near spherical Si particles in the Al matrix. The average particle size and aspect ratio of Si particles of the FSPed samples are observed as 3.7 m and 1.5 m, respectively. which is much smaller than that of cast alloy. The micro porosity has drastically reduced from 10% to 0.76% in the FSPed material as compared to cast alloy.

Cast LM25 alloy is an age hardenable alloy which has the ability to strengthen due to age hardening effect. The effect of ageing time on hardness of as received cast alloy and FSPed alloy at the ageing temperature of 170 ◦ C as shown in Fig.19

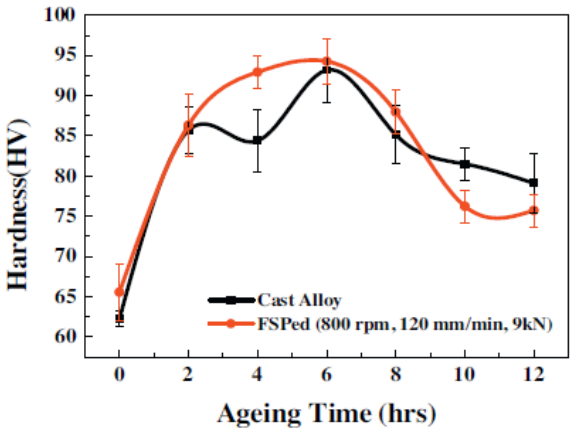

Fig.19. Microhardness of cast and FSPed LM25 alloys at age hardening temperature 170 ◦ C.

The observed trend of age hardening response of FSPed alloy from Fig. 19 is exactly similar to that of as received cast alloy. The hardness values of both of the materials (cast alloy and FSPed alloy) has increased with ageing time up to 6 h and then sharply decreased. The peak ageing conditions for both FSP and cast alloy materials are observed at the ageing temperature of 170 ◦ C for 6 h. the as received cast alloy has been subjected to solution treatment at 520 ◦ C for 8 h prior to age hardening treatment in order to dissolve all the second phase particles in to the aluminum matrix for enhancing age hardening response during post ageing treatment. . The similar age hardening trend of FSPed alloy and as received cast alloy indicates the complete dissolution of second phase particles during FSP. The rapid dissolution kinetics of second phase in the FSPed alloy as com-pared to the as received cast alloy is due to significant severe plastic deformation during friction stir processing with a strain rate of 10 to 10^3 $s^{-1}$and strain level up to 40. The results show that the FSPed alloy has a higher Vickers hardness value than the cast alloy which is shown in Fig. 19. The reason for decrease in hardness of both of the materials above 6 h is due to over ageing effect.

After identification of peak ageing condition for both cast and FSPed alloy ,the same peak ageing treatment was applied to the tensile samples of both cast and FSPed alloys. from now onwards, the cast alloy subjected to solution treatment and then peak aging will be termed as T6 treated cast alloy. The tensile properties of cast, T6 treated cast, FSPed, FSPed + peak aged materials is shown in Fig. 20.

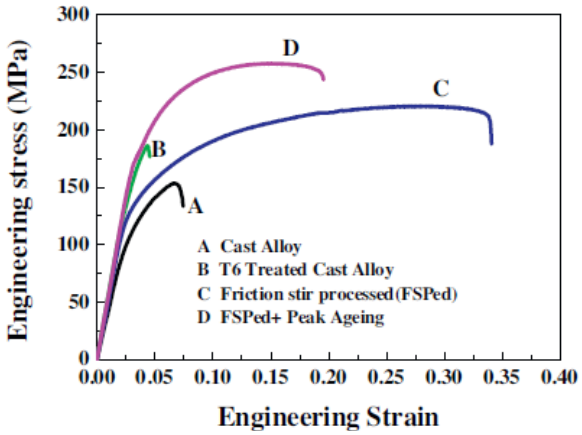

Fig. 20. Stress–strain response of cast alloy, T6 Heat treated cast alloy, FSPed alloy and FSPed + peak aged alloy

As compared to cast alloy, the yield strength (YS), ultimate tensile strength (UTS), uniform elongation (UE) and ductility of FSPed alloy is significantly higher. A significant improvement of mechanical properties in FSPed alloy (UE: 7.7 times, Ductility: 6 times, YS: 12.3% and UTS: 43.7%) as compared to cast alloy is mainly due to the elimination of porosities, refinement of the microstructure, homo-geneously distribution of second phase particles with low aspect ratio. The fracture surfaces of tensile specimens of cast and FSPed alloys before and after peak ageing treatment were examined in a SEM to understand the failure mechanisms Fig. 21.

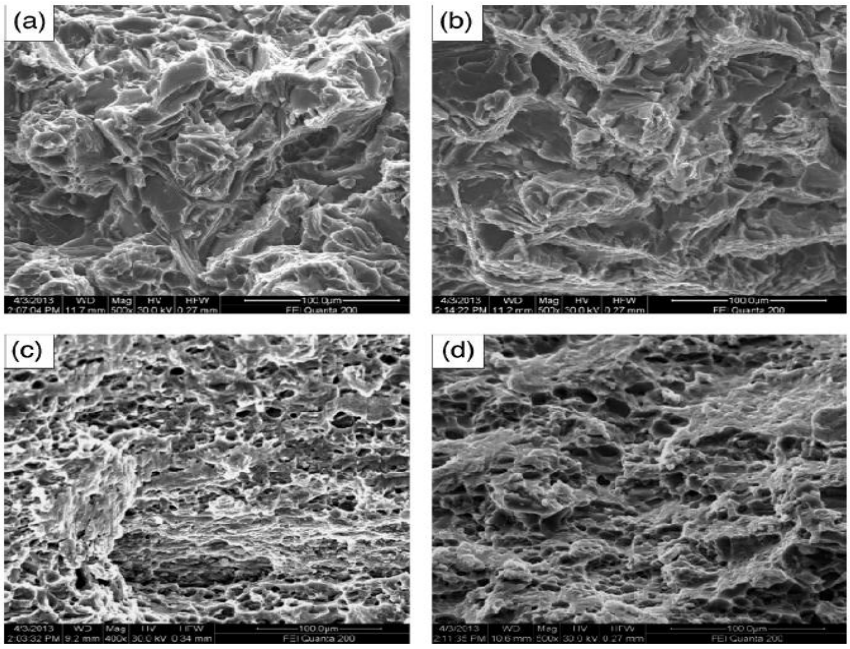

International Journal of Engineering and Manufacturing Science.
ISSN 2249-3115 Volume 7, Number 2 (2017), pp. 203-224

http://www.ripublication.com

Fig. 21. SEM morphology of tensile fracture surface of (a) cast alloy (b), T6 heat treated cast alloy (c) FSPed alloy, and (d) FSPed + peak aged alloy.

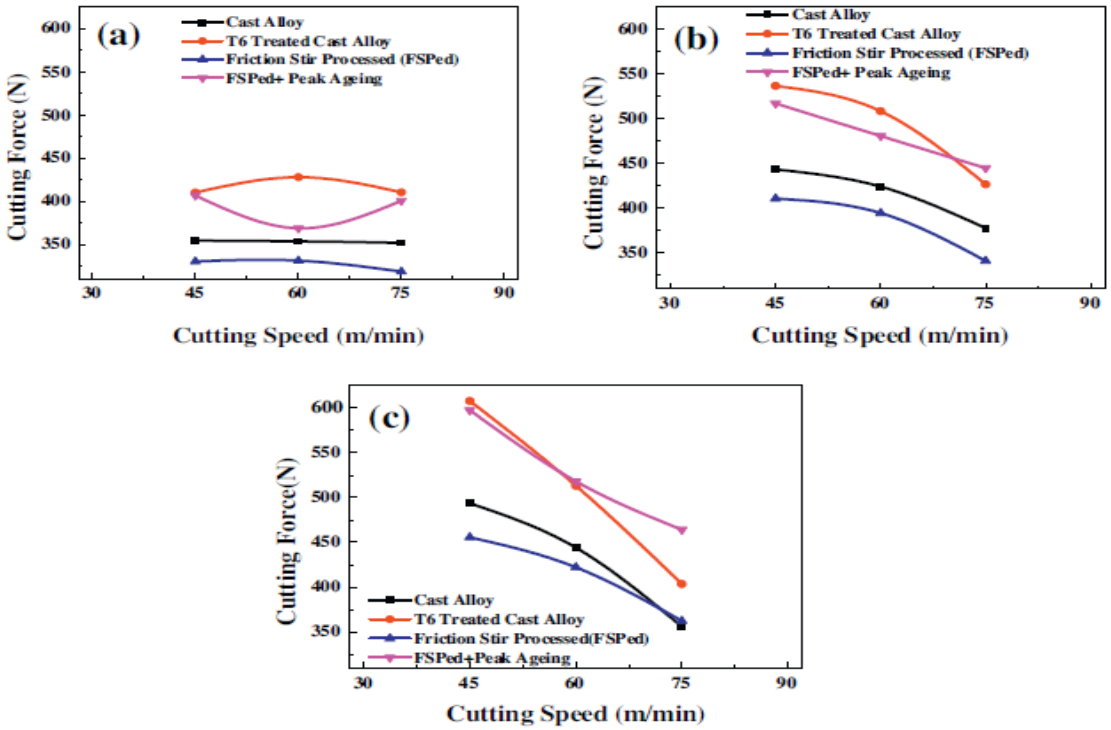

Fig. 22. Effect of cutting speed on cutting force of cast alloy, T6 treated cast alloy, FSPed alloy and FSPed + peak aged alloy at different feed rates: (a) 0.15 mm/rev, (b) 0.2 mm/rev, (c) 0.25 mm/rev.

Fig. 21(a) shows the fracture surface of the as-cast alloy. The flat appearance of the surface confirms the cleavage mode of fracture in the as cast alloy; results in low ductility. Similar features in Fig. 21(b) were also observed in the T6 treated cast alloy which resulted low ductility. In case of FSPed alloy, a slant fracture surface with dimple rupture pattern was observed in Fig. 21(c). The fracture surface of the FSPed + peak aged alloy showed dimple pattern of failure as like FSPed alloy (Fig. 8(d)). The dimple pattern in fracture surface generally gives the indication of ductile material [37,38].

The ease with which a metal can be machined to an acceptable surface finish is generally referred as machinability. The commonly used machinability index is tool life, surface finish, cutting temperature, cutting forces and power consumption.

surface roughness and cutting forces are used as machinability index of the cast and FSPed alloys before and after peak ageing treatment at selected conventional machining parameters. Fig. 22 shows the effect of drilling speed on cutting force of as-cast, T6 treated cast, FSP and FSP + peak aged samples at different feed. At all the cutting speeds and feed, the cutting force observed is lower in FSPed alloys (with or without ageing treatment) than that of similar treated cast alloy. It indicates higher machinability in FSPed alloys than that of cast alloy in both with and without ageing conditions. , the cast alloy has brittle Fe rich intermetallic compound, coarse acicular hard Si particles and brittle -Al dendrites. Therefore while drilling, higher cutting force is required to machine these hard constituents in the cast material. Fig 23 shows the surface roughness of drilled hole for all samples. The FSPed alloys showed lower surface roughness than the cast alloys (Fig. 23) with short discontinuous chips. The temperature induced during drilling of FSPed alloys may be comparatively lower than cast alloy due to absence of (i) brittle Fe rich intermetallics and (ii) network of -Al dendrites. The induced temperature may not be enough to form long continuous chips and hence resulted in formation of discontinuous chips. hence The machinability response (lower cutting force and higher sur-face finish) of FSPed alloy showed higher than that of cast alloy.

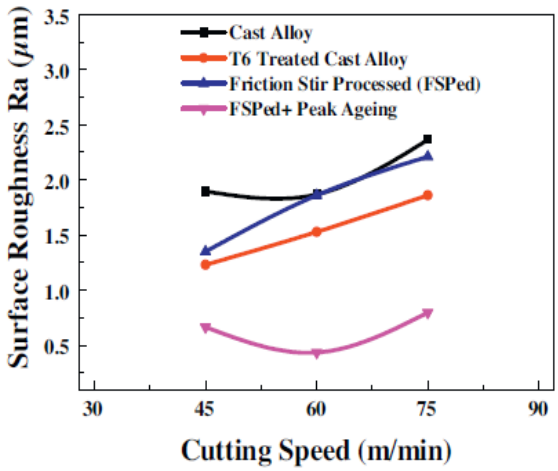

Fig. 23. Effect of cutting speed on surface roughness of drilled hole for cast alloy, T6 treated cast alloy, FSPed alloy and FSPed + peak aged alloy at feed rate of 0.20 mm/rev.

CONCLUSION

It has been discussed all in the literature that the FSP technique can be used as a potential method to fabricate surface MMCs in solid state itself. Being difficult to process materials, aluminium and its alloys can also be easily processed using FSP to produce surface composites of different composition. as processing parameters such

as tool rotational and travel speeds, play an important role in developing defect free stir zone in friction stir processing of aluminium alloys. fabrication of surface composites by FSP is greatly influenced by these parameters and therefore the processing parameters need to be optimized for every individual material system. Grain refinement, improved fatigue properties , microhardness, tensile strength, mechanical properties, mechanical behavior, improved thermal conductivity, machinability and ductility are some of the common observations in all of the aluminium based composites produced by FSP. Apart from these, need to improve wear and corrosion resistant for different Al alloys by FSP. It is expected that composites of other aluminium alloys also will be developed by FSP in future for a wide range of applications.

REFERENCES

[1] D.D.L. Chung, Composite Materials Science and Applications, 2nd ed., Springer, New York, 2010.
[2] J. Hashim, L. Looney, M.S.J. Hashmi, J. Mater. Process. Technol. 92Ð93 (1999) 1Ð7.
[3] M.R. Ghomashchi, A. Vikhrov, J. Mater. Process. Technol. 101 (1999) 1Ð9.
[4] T.M. Yue, G.A. Chadwick, J. Mater. Process. Technol. 58 (1996) 302Ð307.
[5] T.R. Vijayaram, S. Sulaiman, A.M.S. Hamouda, M.H.M. Ahmad, J. Mater. Process. Technol. 178 (2006) 34Ð38.
[6] E.J. Lavernia, N.J. Grant, Mater. Sci. Eng. *A* 98 (1998) 381Ð394.
[7] B.S.S. Daniel, V.S.R. Murthy, G.S. Murty, J. Mater. Process. Technol. 68 (1997) 132Ð155.
[8] A.K. Ghosh, Fundamentals of Metal Matrix Composites, Butterworth-Hinemann, Stoneham, MA, 1993.
[9] E.A. Davis, I.M. Ward, An Introduction to Metal Matrix Composites, Cambridge University Press, New York, USA, 1993.
[10] W.H. Hunt, Processing and Fabrication of Advanced Materials, the Minerals and Metal Materials Society, Warrendale, PA, 1994.
[11] C. Nikhilesh, K.C. Krishan, Metal Matrix Composites, 2nd ed., Springer, New York, 2013.
[12] X. Guo, B. Derby, Prog. Mater. Sci. 39 (1995) 411Ð495.
[13] M.K. Surappa, J. Mater. Process. Technol. 63 (1997) 325Ð333.
[14] R.K. Singh, D.R. Gilbert, J. Fitz-Gerald, D.G. Lee, Surf. Eng. 13 (5) (1997) 389Ð392.
[15] X.H. Wang, M. Zhang, B.S. Du, Mater. Manuf. Process. 28 (5) (2013) 509Ð513.
[16] P.K. Farayibi, J.A. Folkes, A.T. Clare, Mater. Manuf. Process. 28 (5) (2013) 514Ð518.

[17] J.D. Ayers, T.R. Tucker, Thin Solid Film 73 (1) (1980) 201Ð207.
[18] A. Weisheit, G. Galun, B.L. Mordike, S. Hashmi (Ed.), Comprehensive Materials Processing, Elsevier, USA, 2014.
[19] M. Riabkina-Fishman, E. Rabkin, P. Levin, N. Frage, M.P. Dariel, Mater. Sci. Eng. A 302 (2001) 106Ð114.
[20] S. Tailor, R.M. Mohanty, V.K. Sharma, P.R. Soni, Surf. Eng. (2014) <http://dx.doi.org/10.1179/1743294414Y.0000000391>.
[21] G. Madhusudhan Reddy, K. Srinivasa Rao, T. Mohandas, Surf. Eng. 25 (1) (2009) 25Ð30.
[22] G. Madhusudhan Reddy, K. Satya Prasad, K.S. Rao, T. Mohandas, Surf. Eng. 27 (2) (2011) 92Ð98.
[23] R.S. Mishra, Z.Y. Ma, Mater. Sci. Eng. R 50 (2005) 1Ð78.
[24] J.J.S. Dilip, S. Babu, S. Varadha Rajan, K.H. RaÞ, G.D. Janaki Ram, B.E. Stucker, Mater. Manuf. Process. 28 (2) (2013) 189Ð194.
[25] B. Li, Y. Shen, L. Lei, W. Hu, Mater. Manuf. Process. 29 (4) (2014) 412Ð417.
[26] B. Li, Y. Shen, W. Hu, Mater. Manuf. Process. 29 (4) (2014) 493Ð 497.
[27] V. Sharma, U. Prakash, B.V. Manoj Kumar, J. Mater. Process. Technol. 224 (2015) 117Ð134.
[28] Murray J, Peruzzi A, Abriata JP. The Al–Zr (aluminium– zirconium) system. J Phase Equilibria 1992;13(3):277–91.
[29] Yin Z, Pan Q, Zhang Y, Jiang F. Effect of minor Sc and Zr on the microstructure and mechanical properties of Al–Mg based alloys. Mater Sci Eng A Struct Mater Prop Microstruct Process 2002;280:151–5.
[30] Deschamps A, Brechet Y. Influence of quench and heating rates on the ageing response of an Al–Zn–Mg–(Zr) alloy. Mater Sci Eng A Struct Mater Prop Microstruct Process 1998;251:200–7.
[31] Balandin, A. A., Ghosh, S., Bao, W., Calizo, I., Teweldebrhan, D., and et al., "Superior Thermal Conductivity of Single-Layer Graphene," Nano Letters, Vol. 8, No. 3, pp. 902-907, 2008.
[32] Chen, J. H., Jang, C., Xiao, S., Ishigami, M., and Fuhrer, M. S., "Intrinsic and Extrinsic Performance Limits of Graphene Devices on SiO2," Nature Nanotechnology, Vol. 3, No. 4, pp. 206-209, 2008.
[33] Lee, C., Wei, X., Kysar, J. W., and Hone, J., "Measurement of the Elastic Properties and Intrinsic Strength of Monolayer Graphene," Science, Vol. 321, No. 5887, pp. 385-388, 2008.
[34] Stankovich, S., Dikin, D. A., Dommett, G. H., Kohlhaas, K. M., Zimney, E. J., and et al., "Graphene-Based Composite Materials," Nature, Vol. 442, Paper No. 7100, pp. 282-286, 2006
[35] Novoselov, K. S., Geim, A. K., Morozov, S., Jiang, D., Zhang, Y., and et al., "Electric Field Effect in Atomically Thin Carbon Films," Science, Vol. 306, No. 5696, pp. 666-669, 2004.

[36] Barmouz, M. and Givi, M. K. B., "Fabrication of in Situ Cu/SiC Composites using Multi-Pass Friction Stir Processing: Evaluation of Microstructural, Porosity, Mechanical and Electrical Behavior," Composites Part A: Applied Science and Manufacturing, Vol. 42, No. 10, pp. 1445-1453, 2011.

[37] Panigrahi SK, Jayaganthan RJ. Development of ultrafine grained high strength age hardenable Al 7075 alloy by cryorolling. Mater Des 2011;32(6):3150–60.

[38] Panigrahi SK, Yuan W, Mishra RS, DeLorme R, Davis B, Cho K. A study on the combined effect of forging and aging in Mg–Y–RE alloy. Mater Sci Eng: A 2011;530:28–35.